Subunit composition of a bicomponent toxin: Staphylococcal leukocidin forms an octameric transmembrane pore

GEORGE MILES,[1,3] LIVIU MOVILEANU,[1,3] AND HAGAN BAYLEY[1,2]

[1]Department of Medical Biochemistry and Genetics, The Texas A&M University System Health Science Center, College Station, Texas 77843–1114, USA
[2]Department of Chemistry, Texas A&M University, College Station, Texas 77843–3255, USA

(RECEIVED October 25, 2001; FINAL REVISION December 18, 2001; ACCEPTED December 18, 2001)

Abstract

Staphylococcal leukocidin pores are formed by the obligatory interaction of two distinct polypeptides, one of class F and one of class S, making them unique in the family of β-barrel pore-forming toxins (β-PFTs). By contrast, other β-PFTs form homo-oligomeric pores; for example, the staphylococcal α-hemolysin (αHL) pore is a homoheptamer. Here, we deduce the subunit composition of a leukocidin pore by two independent methods: gel shift electrophoresis and site-specific chemical modification during single-channel recording. Four LukF and four LukS subunits coassemble to form an octamer. This result in part explains properties of the leukocidin pore, such as its high conductance compared to the αHL pore. It is also pertinent to the mechanism of assembly of β-PFT pores and suggests new possibilities for engineering these proteins.

Keywords: β barrel; leukocidin; membrane protein; pore-forming toxin; protein–protein interaction; staphylococcal α-hemolysin; subunit stoichiometry

The β-barrel pore-forming toxins (β-PFTs) are a family of polypeptides that are related by sequence and structure (Song et al. 1996; Gouaux et al. 1997; Olson et al. 1999; Pédelacq et al. 1999; Heuck et al. 2001). β-PFTs are secreted by bacteria as water-soluble monomers, which bind to the surfaces of susceptible cells and assemble into transmembrane pores leading to cell permeation and lysis (Alouf and Freer 1999; Bhakdi et al. 2000; Menestrina et al. 2001). Staphylococcal α-hemolysin (αHL), a β-PFT comprising a single polypeptide of 293 amino acids, has been studied in great detail (Gouaux 1998; Bhakdi et al. 2000). The crystal structure of the heptameric pore formed by αHL in detergent has been determined at 1.9-Å resolution (Song et al. 1996). The pore has also been shown to be a heptamer on erythrocyte membranes (Gouaux et al. 1994), in planar lipid bilayers (Krasilnikov et al. 2000) and supported bilayers (Fang et al. 1997), and after spontaneous assembly in solution (Cheley et al. 1997). It remains conceivable that a small fraction of the αHL pore is a hexamer (Czajkowsky et al. 1998). The protein has been subjected to extensive structure-function investigations by mutagenesis and targeted chemical modification. This work has shed light both on the assembly process (Walker et al. 1995; Cheley et al. 1997; Olson et al. 1999) and the properties of the assembled pore (Braha et al. 1997; Movileanu et al. 2000; Howorka et al. 2001). The significance of αHL as a pathogenic factor has also been examined (Bhakdi et al. 2000), and engineered αHL pores are emerging as useful tools in biotechnology (Eroglu et al. 2000; Bayley and Cremer 2001).

On the whole, the leukocidins have been less thoroughly investigated at the molecular level. Like αHL, the leukocidins have been implicated as virulence factors, primarily in wounds and infections of soft tissues (König et al. 1997; Alouf and Freer 1999). Both components of these binary toxins are in the β-PFT family. There are at least five

Reprint requests to: Hagan Bayley, Department of Medical Biochemistry and Genetics, The Texas A&M University System Health Science Center, College Station, TX 77843-1114, USA; e-mail: bayley@tamu.edu; fax: (979) 847-9481.

[3]These authors contributed equally to this work.

Article and publication are at http://www.proteinscience.org/cgi/doi/10.1110/ps.4360102.

 Copyright © 2002 The Protein Society

class-F components that share 71%–79% identity at the amino acid level and six class-S components that share 59%–79% identity (Gouaux et al. 1997; Alouf and Freer 1999). The extent of sequence identity between members of one class and members of the other is 20%–30%. No member of either class is >30% identical to αHL (Fig. 1A). Regions of similarity are dispersed throughout the aligned polypeptides (Fig. 1B). The structures of the water-soluble monomeric forms of two class-F components, LukF (HlgB) and LukF-PV, were determined recently (Olson et al. 1999; Pédelacq et al. 1999). Excluding the stem and N-terminal latch domains, both polypeptides display folds that closely resemble the fold of an individual protomer in the fully assembled αHL pore (Fig. 1C). The majority of strictly conserved residues in αHL, LukF, and LukS are clustered within the hydrophobic core of the structure and are most likely required to preserve the fold. Together the structures of the LukF monomers and the αHL heptamer serve as

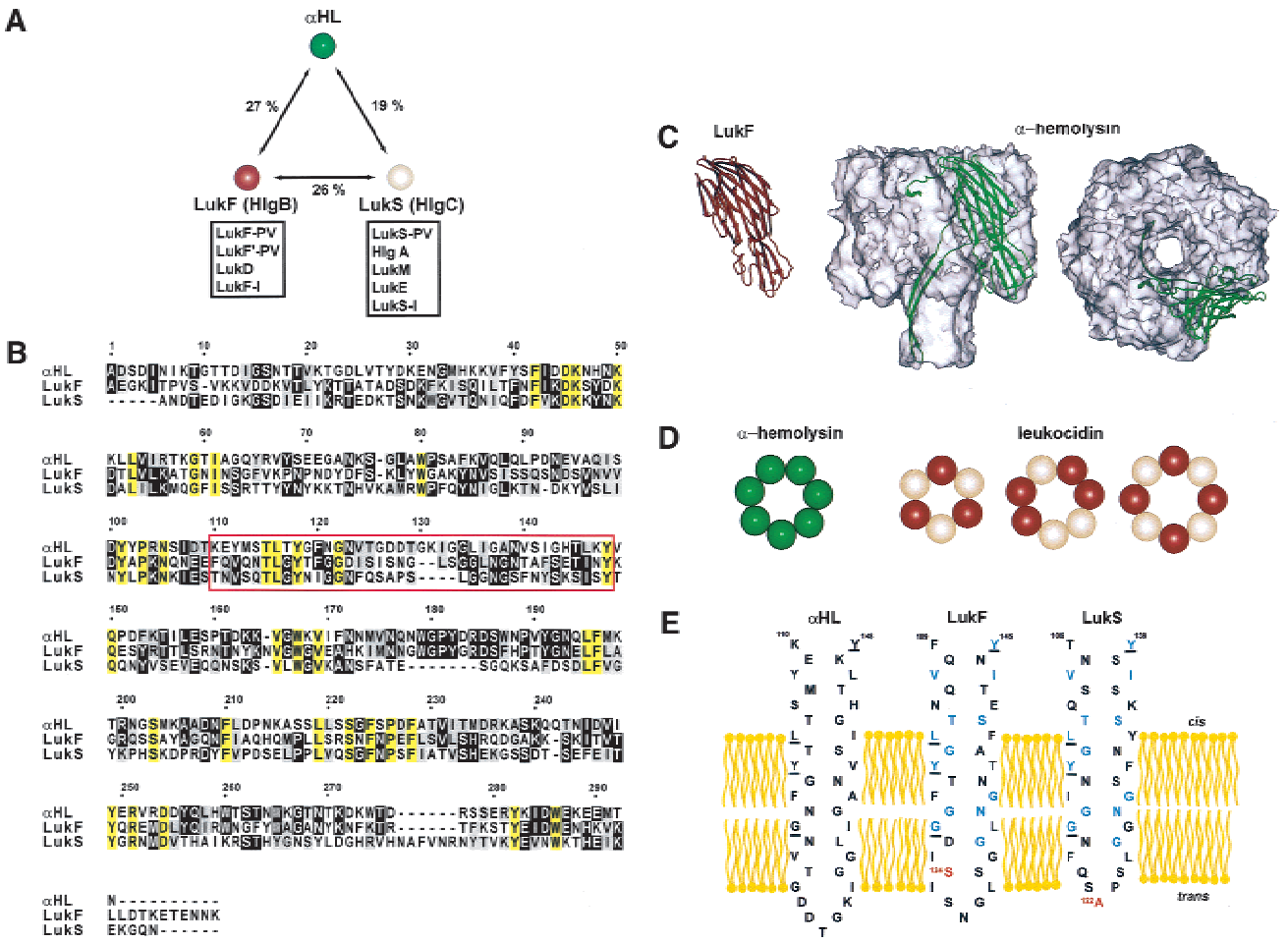

Fig. 1. Relationships between α-hemolysin (αHL) and leukocidin, members of the β-barrel pore-forming toxins (β-PFT) family. (*A*) Percent amino acid identity between αHL, LukF (HlgB), and LukS (HlgC). Other members of the F and S classes of leukocidin subunits are listed in the boxes. Within class F the proteins share 71%–79% identity and within class S 59%–79% identity. (*B*) Primary sequence alignment of αHL, LukF (HlgB), and LukS (HlgC). Identical and conserved residues are highlighted in black and gray, respectively. Residues that are identical in all three proteins are indicated with a yellow background. The residues of αHL that are located in the transmembrane β barrel, as well as the residues of LukF and LukS presumed to be in the barrel, are enclosed in the red box. The figure was generated using Clustal W 1.74 (Thompson et al. 1994). (*C*) Crystal structures of the LukF monomer (1LKF.pdb) and the αHL heptamer (7AHL.pdb). The secondary structure of one protomer of αHL is shown in green for comparison with LukF (maroon). The remainder of the heptamer is shown in a molecular surface representation generated by SPOCK 6.3 (Christopher 1998) and rendered using Raster3D (Merritt and Murphy 1994). (*D*) Possible subunit stoichiometries for the leukocidin pore. LukF and LukS are illustrated as maroon and tan spheres. The homoheptameric αHL is shown for comparison. (*E*) Schematic representation of the antiparallel β strands forming the β barrel of αHL and the corresponding residues of LukF and LukS. The residues are portrayed as either facing the lipid bilayer (exterior) or lining the lumen of the pore (interior). Identical residues are underscored, and identities between LukF and LukS are colored blue. Residues in red were mutated to cysteine (S124 in LukF and A122 in LukS) for modification by MTSES. The *cis* and *trans* sides of the bilayer are marked.

prototypes for the beginning and end points of β-PFT assembly (Olson et al. 1999; Pédelacq et al. 1999; Heuck et al. 2001).

Limited data exist on the mechanism of assembly and molecular architecture of the leukocidin pore. No structural information is available for a LukS monomer nor for an assembled leukocidin oligomer. Previous studies have suggested that the pore contains LukF and LukS in a molar ratio of 2:1 or 1:1 and that it has an internal diameter of 1.9 –2.4 nm, as estimated from osmotic protection experiments and electron microscopy (Ozawa et al. 1995; Kaneko et al. 1997; Sugawara et al. 1997, 1999; Ferreras et al. 1998). Based on these observations, several groups have speculated that the leukocidin oligomer is a hexamer (Sugawara et al. 1997, 1999; Ferreras et al. 1998; Pédelacq et al. 1999). Other possibilities include the formation of heteromers consisting of 4:3 or 3:4 mixtures of LukF and LukS or larger complexes (Fig. 1D). Recently, it was shown that a leukocidin pore has a unitary conductance of 2.5 ns in 1 M KCl (Miles et al. 2001). As this value is over three times greater than the conductance of αHL, the diameter of the leukocidin pore can be estimated to be nearly twice that of αHL, arguing in favor of more than six subunits. However, it is possible that the large conductance of the leukocidin pore arises from the lack of side chains equivalent to those in the central constriction of αHL: Glu 111, Lys 147, and Met 113 (Fig. 1E). To settle this question, we have determined the subunit composition of the leukocidin pore formed by the class-F component HlgB (here LukF; Cooney et al. 1988, 1993) and the class-S component HlgC (here LukS; Cooney et al. 1988, 1993).

Results and Discussion

Subunit composition of leukocidin by gel-shift electrophoresis

We found that both LukF and LukS are able to tolerate large extensions on their C termini. We exploited this observation to determine the subunit composition of the leukocidin oligomer by gel-shift electrophoresis (Gouaux et al. 1994). *Bacillus cereus* hemolysin II (HlyII) and its close relatives contain a naturally occurring C-terminal extension of 94 amino acids, which shares no homology with the other β-PFTs. The mutants LukF-TL and LukS-TL were constructed in which the *Bacillus* tail was spliced onto the respective C termini. The properties of these constructs were largely unchanged as ascertained by hemolytic activity and the stabilities in SDS of the oligomers formed from them (data not shown).

The *Bacillus* tail does alter the electrophoretic mobility of leukocidin oligomers enough to permit separation of heteromeric pores with differing subunit combinations. Oligomers containing various ratios of LukF to LukF-TL with wild-type LukS were obtained by cotranslation in the presence of rabbit erythrocyte membranes. The concentration of LukS plasmid in the translation was equal to the total concentration of LukF and LukF-TL plasmids. At least a fraction of leukocidin oligomers are stable in SDS (Sugawara et al. 1997; Miles et al. 2001), and analysis by SDS-polyacrylamide gel electrophoresis and autoradiography revealed five bands (Fig. 2A). Each increment in electrophoretic mobility must correspond to the incorporation of one LukF-TL subunit into the oligomeric complex. The fastest migrating band represents the native SDS-stable leukocidin oligomer containing only LukF and LukS subunits; whereas the band of lowest mobility represents the leukocidin oligomer containing LukF-TL and LukS. Therefore, the three additional bands, in order of decreasing mobility, represent heteromers containing one, two, and three LukF-TL subunits. The result indicates that the leukocidin oligomer contains four LukF subunits.

To assess the contribution of LukS to the leukocidin oligomer, the complementary experiment was performed in which oligomers were assembled from LukS, LukS-TL, and LukF. Again, five oligomeric species were resolved by gel electrophoresis (Fig. 2B). In this case, the result indicates that the leukocidin oligomer contains four LukS subunits. Taken together, the electrophoresis experiments show that the leukocidin pore is an octamer consisting of four subunits of Luk F and four subunits of LukS (Fig. 2C).

The gel-shift experiments are certainly not as clean as those performed previously with αHL (Gouaux et al. 1994; Braha et al. 1997). However, leukocidin oligomers are more difficult to form and to handle, and the clarity of the bands could not be improved, even though a wide range of experimental variations were tested, including several different N- and C-terminal extensions and numerous conditions for electrophoresis. Gel-shift experiments involving all four constructs, LukF, LukF-TL, LukS, and LukS-TL, lacked sufficient resolution for individual bands to be distinguished (data not shown).

Subunit composition of leukocidin by targeted chemical modification and single-channel recording

An independent method was used to elucidate the subunit composition of the leukocidin pore. Cysteine residues were engineered with side chains projecting into the presumed lumen (Fig. 1E) and reacted with the sulfhydryl-specific reagent MTSES (sodium (2-sulfonatoethyl)methanethiosulfonate) during single-channel recording in planar bilayers. In the case of cysteine substitutions near the *trans* mouth of the transmembrane barrel (Fig. 1E), distinct current steps were obtained with MTSES, but mutations at several other positions and alternative reagents gave less favorable results. The voltage-dependent gating of the leukocidin pore differs from that of αHL. At positive potentials, above +40

mV, a complex gating profile is seen (Miles et al. 2001). Further, the single-cysteine mutants used here gate at potentials more negative than −80 mV. Therefore, experiments were performed at a holding potential of −60 mV, at which the pores remain open for long periods and carry sufficient current to permit detection of the modifications.

Single-channel recordings were performed on gel-purified leukocidin oligomers containing LukF-S124C and wild-type LukS (Fig. 3A). The unitary conductance was 2420 ± 100 pS (n = 12). When MTSES (1.5 mM) was added to the *trans* side of the lipid bilayer, a stepwise decrease in the current was seen (Fig. 3A). Four clearly resolved levels were observed, with an average step blockade of 3.5 ± 0.7 pA or 2.4% ± 0.4% (n = 12; Table 1). In 11 of 12 experiments, four steps only were observed over the course of ~5 sec; no further events were seen in the next 45 min. In one case, three events were observed. The cysteine modification could be reversed in a stepwise fashion by the addition of DTT (10 mM; Fig. 3A). The results confirm that the leukocidin oligomer contains four LukF subunits.

Similarly, single-channel recordings were made with leukocidin oligomers containing LukS-A122C and wild-type LukF (Fig. 3B). The unitary conductance was 2560 ± 90 pS (n = 9). Again, four clearly resolved steps to lower conductance were observed upon addition of MTSES (1.5 mM) to the *trans* chamber, in this case in all nine experiments. The average step size was 3.3 ± 0.6 pA or 2.1% ± 0.3% (n = 9; Table 1). Again, the cysteine modification could be reversed in stepwise fashion by the addition of DTT (10 mM; Fig. 3A). The results confirm that the leukocidin oligomer also contains four LukS subunits.

The total current blockade produced by MTSES modification of the cysteine-substituted leukocidin pores was investigated at the macroscopic current level. For LukF-S124C/wild-type LukS and wild-type LukF/LukS-A122C, the values were 9.9% ± 1.2% (n = 4) and 8.5% ± 0.7% (n = 4), respectively (Fig. 4; Table 1). These results are consistent with the total extent of block seen in the single-channel experiments, suggesting that the majority of leukocidin pores in a population are octamers containing four LukF subunits and four LukS subunits, in agreement with the gel-shift experiments.

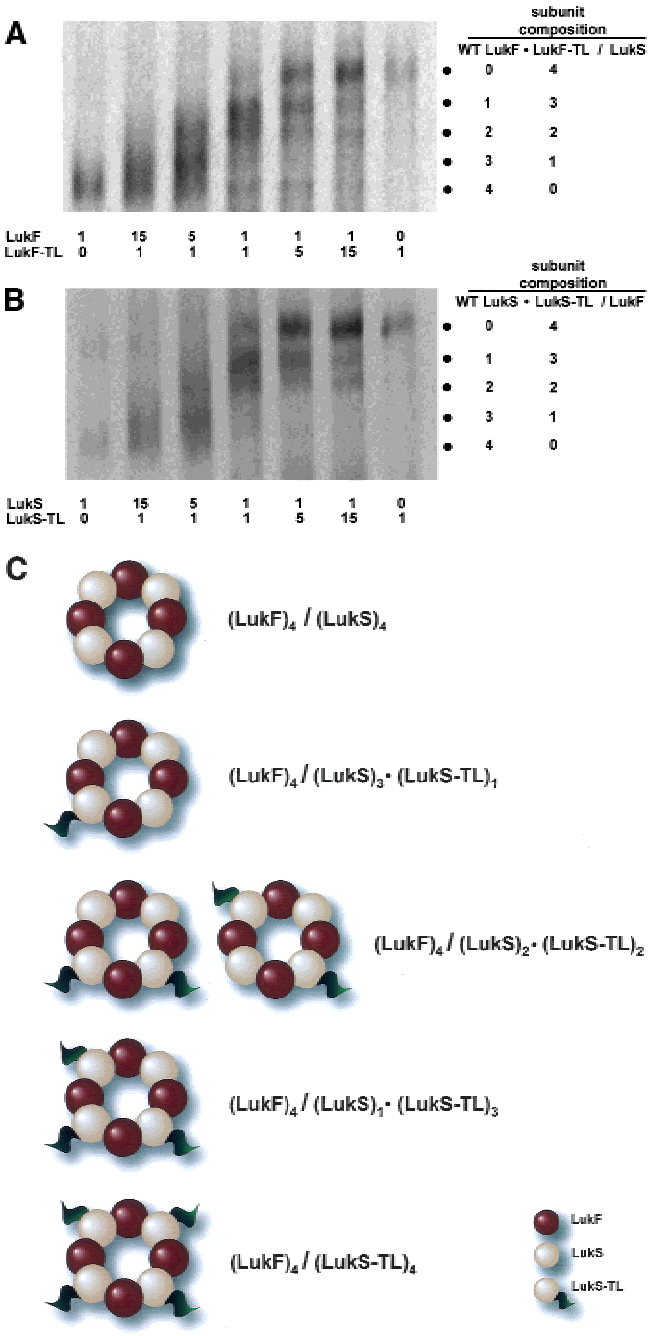

Fig. 2. Assembly and separation of leukocidin heteromers. (*A*) Separation of heteromers formed from wild-type LukS, wild-type LukF, and LukF-TL by SDS-polyacrylamide gel electrophoresis. [^{35}S]Methionine-labeled wild type and mutant leukocidin polypeptides were synthesized in vitro by coupled transcription and translation and assembled into heteromers by including rabbit erythrocyte membranes. The concentration of LukS plasmid in the translation was equal to the total concentration of wild-type LukF and LukF-TL plasmids. The LukF and LukF-TL DNAs were mixed in the ratios indicated under the lanes. Washed membranes were solubilized in sample buffer without heating and subjected to electrophoresis in a 5% gel. An autoradiogram exposed overnight is shown. The black dots indicate the five bands that were formed. The deduced subunit compositions are listed to the right. (*B*) Heteromer formation from wild-type LukF and various ratios of wild-type LukS to LukS-TL, performed as described in panel *A*. The experiments in *A* and *B* were reproduced at least five times each. (*C*) Graphical representations of the leukocidin oligomers inferred from the results in *B*. All possible heteromeric permutations resulting from the mixtures of wild-type LukF with LukS and LukS-TL are illustrated.

Previous applications of the approaches used here

Both techniques applied here for counting subunits in a channel or pore have been used before, but neither has been

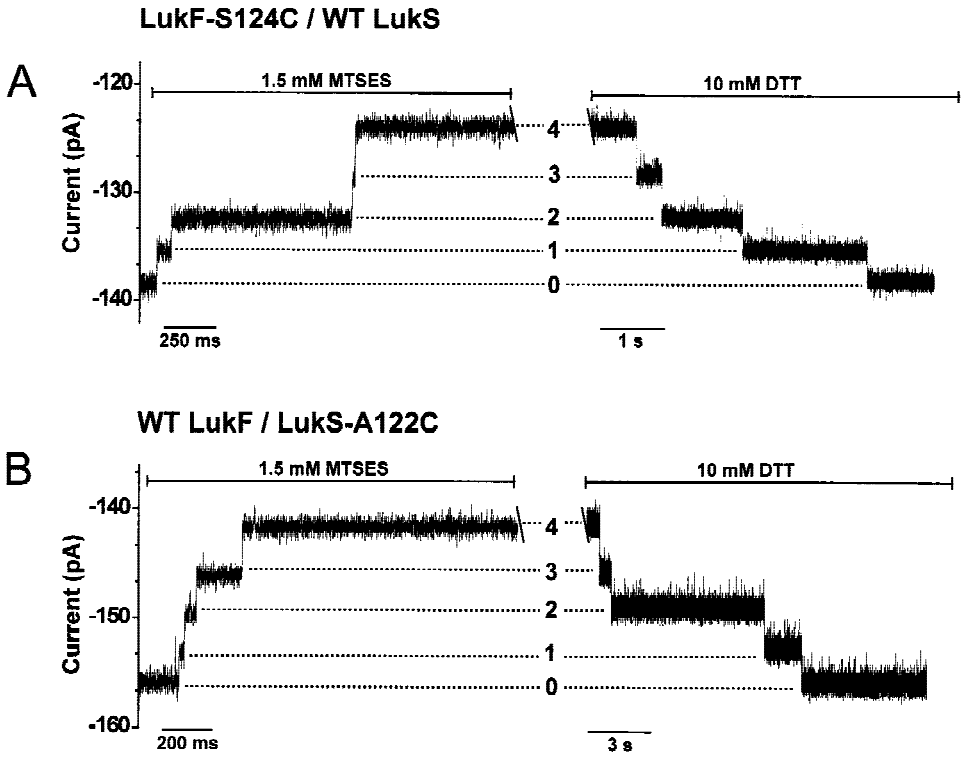

Fig. 3. Representative single-channel recordings of cysteine-substituted leukocidin pores reacting with MTSES. (*A*) LukF-S124C/wild-type LukS; (*B*) wild-type LukF/LukS-A122C. In both single-channel traces, there is a gap of ~45 min between the reaction with 1.5 mM MTSES reagent and the addition of 10 mM DTT. Both reagents were added to the *trans* chamber. The holding potential was −60 mV and the signal was low-passed filtered at 0.5 kHz with a Bessel filter.

applied to a heteromeric membrane protein. The original gel-shift approach was based on a mobility change brought about by site-specific chemical modification and was used to count the seven subunits of the homomeric αHL pore (Gouaux et al. 1994; Braha et al. 1997). Gel-shift experiments based on genetically engineered truncations or extensions have proved useful in other cases (Heginbotham et al. 1997; Zitzer et al. 1999; Miyata et al. 2001), and this approach was adopted here. However, it was not possible to count all the subunits in a single experiment because the leukocidin oligomers are more difficult to form and to separate. Therefore, the LukF and LukS subunits were counted separately, which in any case led to a complete description of the stoichiometry. Similarly, it was difficult to count all the subunits at once in the bilayer experiments. In experiments with oligomers in which both components were mutated (LukF-S124C/LukS-A122C), we performed one experiment with seven steps, four with six steps, and one with five steps (data not shown). Krasilnikov and colleagues experienced similar difficulties in examining the αHL heptamer, in which only 9 out of 38 counts were complete (Krasilnikov et al. 2000), perhaps because of steric or coulombic repulsion between the incoming reagent and the residues modified initially. Therefore, the LukF and LukS subunits were again counted separately and 20 out of 21 experiments revealed four subunits, which we believe to be the full count in each case.

Permutation of the subunits about the central axis

The experiments performed here do not reveal the arrangement of the LukF and LukS subunits around the central axis. In the absence of additional information, we favor the simplest scheme in which LukF and LukS alternate (Fig. 5). This arrangement requires only two types of subunit–subunit interaction; whereas all other arrangements and random assortment generate four different interfaces. Unless a structure of the pore can be determined, resolution of this question will require cross-linking experiments or visualization by electron or atomic force microscopy. It can be noted that both possibilities have been found in membrane proteins: The α and β subunits of the extramembraneous F_1 portion of ATP synthase alternate around a threefold axis (Abrahams et al. 1994); whereas the α subunits of the nicotinic acetylcholine receptor pentamer ($\alpha_2\beta\gamma\delta$) are in different environments (Karlin 1993).

Table 1. *Effect of the sulfhydryl reagent MTSES on leukocidin pores with cysteine-substituted subunits: single-channel and macroscopic currents*

Pore	LukF-S124C/WT LukS	WT LukF/LukS-A122C
I_s[a]	145 ± 6	154 ± 6
$\Delta I_s(1)$[b]	3.0 ± 0.7	2.8 ± 0.6
$\Delta I_s(2)$[b]	3.3 ± 0.5	3.1 ± 0.5
$\Delta I_s(3)$[b]	3.7 ± 0.4	3.5 ± 0.4
$\Delta I_s(4)$[b]	4.3 ± 0.6	4.0 ± 0.5
$\Delta I_s*(4)$[c]	4.4 ± 0.6	4.1 ± 0.6
$\Delta I_s*(3)$[c]	3.7 ± 0.3	3.3 ± 0.5
$\Delta I_s*(2)$[c]	3.2 ± 0.5	3.2 ± 0.4
$\Delta I_s*(1)$[c]	3.1 ± 0.8	2.8 ± 0.5
$\Sigma\Delta I_s/I_s$[d]	10 ± 1	8.8 ± 0.6
$\Delta I_m/I_m$[e]	9.9 ± 1.2	8.5 ± 0.7

[a] Mean single-channel current in pA (± SD) at −60 mV.
[b] Mean blockade in pA (± SD) after each modification step with MTSES. The numbering of the four steps is the same as shown in Figure 3. All experiments showed four steps except one with Luk F-S124C/WT LukS, in which three steps were seen in 1 of 12 experiments. In the latter experiment, three steps were also seen during the reversal by DTT. For wild-type LukF/LukS-A122C, 9 experiments were done.
[c] Mean increase in current in pA (± SD) after each reversal step by DTT. The numbering of the four steps is the same as shown in Figure 3.
[d] Mean total extent of blockade (% ± SD) in the single-channel experiments after completion of the reaction with MTSES.
[e] Mean total extent of blockade (% ± SD) in the macroscopic current experiments after completion of the reaction with MTSES (for details, see Figure 4).

Prediction of the internal diameter of the leukocidin pore

Because stepwise changes in the single-channel current occur when either subunit is chemically modified, both LukF and LukS must contribute amino acid side chains to the lumen of the transmembrane section of the pore. Therefore, in analogy with the 14-stranded β barrel of αHL, we propose that the transmembrane domain of leukocidin is a 16-stranded β barrel with two strands contributed by each subunit. In the αHL pore, S = N, where S is the shear number (Murzin et al. 1994a) and N the number of β strands (Song et al. 1996). Assuming S = 16 for the leukocidin pore, the calculated diameter (C_α–C_α) is 28 Å (Murzin et al. 1994a,b). By a similar estimation, the diameter of the αHL barrel is 25 Å (Song et al. 1996). A simplistic calculation of the expected ratio of conductance values for the leukocidin and αHL pores can be made based on these values: $D_2^2/D_1^2 = 1.3$. This is far lower than the measured conductance ratio of 3.3 (Miles et al. 2001). Therefore, the increased diameter of the barrel caused by the additional subunit only accounts in part for the increased conductance of the leukocidin pore.

Previous determinations of leukocidin stoichiometry

Previous attempts to determine the ratio of LukF to LukS subunits in the leukocidin pore proved unconvincing. Densitometric data from immunoblots of the oligomeric species provided an estimate of 2:1 for the molar ratio of LukF to LukS (Ozawa et al. 1995; Kaneko et al. 1997). On the other hand, SDS gel electrophoresis of pores purified on sucrose gradients have indicated that the ratio is ~1:1 (Sugawara et al. 1997, 1999; Ferreras et al. 1998). Studies by electron microscopy were inconclusive. Ring-shaped structures have been observed on erythrocyte membranes, and it has been speculated that they are hexamers (Sugawara et al. 1997, 1999). Finally, the pore has been modeled as a hexamer but with little justification (Pédelacq et al. 1999).

Our results suggest that the majority of the SDS-resistant leukocidin pores are octamers, but it remains possible that a small fraction are hexamers or of other stoichiometries. For example, a fraction of αHL pores may be hexamers (Czajkowsky et al. 1998; Bhakdi et al. 2000). Membrane proteins made from large rings of subunits are known to have vari-

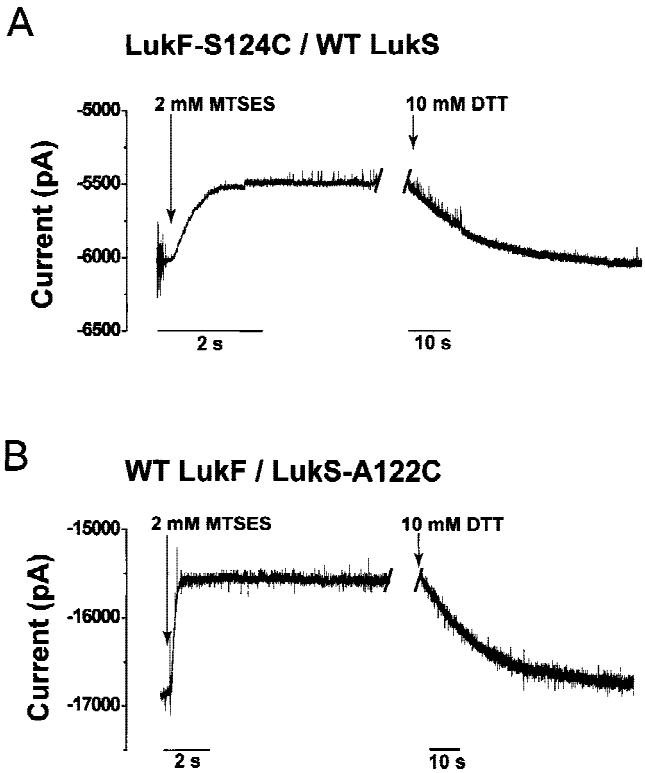

Fig. 4. Typical macroscopic current recordings of leukocidin pores containing cysteine replacements during reaction with 2 mM MTSES added to the *trans* side of the lipid bilayer. (*A*) LukF-S124C/wild-type LukS; (*B*) wild-type LukF/LukS-A122C. In both traces, there is a gap of ~45 min between the addition of MTSES and the reversal of the reaction with 10 mM DTT. The holding potential was −60 mV. The *trans* bath was stirred throughout the experiment. The signal was low-pass filtered at 1 kHz with an 8-pole Bessel filter.

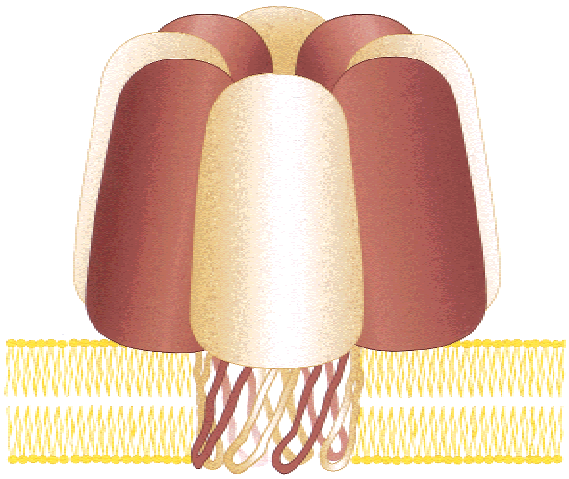

Fig. 5. Model of an octameric staphylococcal leukocidin pore. Both LukF (maroon) and LukS (tan) contribute four subunits as shown here. We suggest that the transmembrane domain of the leukocidin pore is a 16-stranded β barrel.

able numbers of subunits, as in the case of the cholesterol-dependent pore-forming toxins (Bayley 1997; Heuck et al. 2001) or a fixed number of subunits that varies between homologs, as in the case of the F_O domain of ATP synthase (Stock et al. 1999; Seelert et al. 2000; Jiang et al. 2001; Stahlberg et al. 2001). Other proteins with small rings of subunits also have variable numbers of subunits; for example, the Hs1VU protease of *Escherichia coli* can form hexameric and heptameric rings (Rohrwild et al. 1997), and viral capsid proteins can be located in different environments in the same particle, for example around fivefold or pseudo-six-fold axes in T = 3 icosahedra (Harrison 2001).

Evolutionary considerations

It seems likely that the LukF and LukS genes were formed by an ancient duplication (Archibald et al. 2000). The αHL gene, which has a similar extent of sequence identity, must have diverged very soon before or after (Fig. 1A). Presumably, a mutation affecting the interface between the subunits then occurred in one subunit, making it unable to interact with the second. A complementary mutation must have occurred in the second subunit, allowing the first subunit back into the oligomer and fixing the system genetically as a ring of alternating subunits. In accord with this possibility, several F and S genes occur in single transcription units, permitting coordinated regulation of expression (Alouf and Freer 1999; Bronner et al. 2000). Because F and S subunits can mix and match (Prévost et al. 1995), the leukocidin heteromer can display a wide variety of combinations and permutations (Ferreras et al. 1998; Menestrina et al. 2001), which might offer a selective advantage by contributing to the various cellular and species specificities that have been observed (König et al. 1997; Gravet et al. 1998).

Future prospects

Knowledge of the subunit composition of the leukocidin pore raises interesting questions about the assembly process. In the case of αHL, monomers first form a heptameric prepore (Walker et al. 1992, 1995). Nothing is known about intermediates in heptamer formation. For example, in one possibility, the heptamer may assemble through multiple pathways involving random collisions of individual subunits and incomplete oligomers. In a second possibility, the sequential addition of individual subunits may occur until a ring is completed. In the case of the leukocidin pore, it is possible that specific dimers are first formed. Because the prepore-to-pore conversion is the rate-determining step, for αHL at least (Walker et al. 1995), and the intermediates are short-lived, it will be a challenge to settle this issue.

Knowledge of the subunit composition also opens up new prospects for the engineering of β-PFTs. αHL has been a productive target for engineering studies (Bayley 1999; Eroglu et al. 2000; Bayley and Cremer 2001). However, new methods for forming and purifying heteromeric pores had to be developed to circumvent difficulties arising from the presence of seven identical subunits. For example, procedures have been refined for placing single mutations (Braha et al. 1997) or chemical modifications (Movileanu et al. 2000) within the αHL pore. Extensions of these procedures with the leukocidin pore should allow more complex structures to be made involving the modification of two neighboring subunits. It might also be possible to gain control over the number of subunits in a pore by engineering the subunit interfaces.

Materials and methods

Site-directed mutagenesis and fusion proteins

All constructs were made in a T7 expression vector (Cheley et al. 1997) and verified by DNA sequencing. Site-directed mutagenesis was used to create the single-cysteine mutants LukF-S124C and LukS-A122C, as described elsewhere (Howorka and Bayley 1998). Ligation-free in vivo recombination (Jones 1995; Howorka and Bayley 1998) was used to fuse a 3′ extension directly to the last codon of both the *luk*F and *luk*S genes (Miles et al. 2001). The extension encoded the 94 amino acids of the *Bacillus* hemolysin-II C-terminal tail (residues 289–382; Baida et al. 1999). The fused genes were generated in the T7 vector by cotransforming *E. coli* XL-10 Gold cells with PCR products encompassing the *Bacillus* tail and *luk*F or *luk*S.

Analysis of leukocidin hetero-oligomers

Hetero-oligomers of leukocidin subunits containing LukF and/or LukF-TL with LukS and/or LukS-TL were prepared by mixing the DNA constructs in various molar ratios prior to transcription and translation in a cell-free system in the presence of rabbit erythrocyte membranes (Cheley et al. 1999). The washed membrane pellets were solubilized with sample buffer (Laemmli 1970) and subjected to SDS-polyacrylamide gel electrophoresis in a 5% gel. An autoradiogram was made of the dried gel.

Gel-purified leukocidin oligomers

Leukocidin oligomers were prepared by in vitro expression in the presence of rabbit erythrocyte membranes as described above. As a precaution against the oxidation of cysteine residues, 2 mM DDT was added to the buffer used to wash the membrane pellet (Movileanu et al. 2001). The oligomers were purified by SDS-polyacrylamide gel electrophoresis in an 8% gel in the presence of 0.1 mM sodium thioglycolate (Miles et al. 2001; Movileanu et al. 2001). The oligomers were stored at −80°C in 10 mM Tris.HCl at pH 8.0 containing 2 mM DTT.

Electrical recordings

Single-channel recordings were carried out with planar lipid membranes, as described earlier (Montal and Mueller 1972; Braha et al. 1997). Both the *cis* and *trans* chambers of the apparatus contained recording buffer: 1 M KCl, 50 mM Tris.HCl, 200 μM DTT, 100 μM EDTA at pH 8.0. The bilayer was formed from 1,2-diphytanoyl-*sn*-glycerophosphocholine (Avanti Polar Lipids, Inc.). Protein was added to the *cis* chamber, which was at ground. Single-channel and macroscopic currents were recorded by using a patch clamp amplifier (Axopatch 200B, Axon Instruments). A Pentium PC equipped with a DigiData 1200 A/D converter (Axon Instruments) was used for data acquisition. The current traces were low-pass filtered with an 8-pole Bessel-filter (Model 900, Frequency Devices) at 0.5 kHz for single-channel currents and 1 kHz for macroscopic currents, and acquired directly by the computer at a sampling rate of 5 kHz by using Clampex8.0 software (Axon Instruments). Measurements were performed at a temperature of 23° ± 0.5°C. Fresh stock solutions (100 mM) of sodium (2-sulfonatoethyl)methanethiosulfonate (MTSES, Toronto Research Chemicals) in recording buffer without DTT were prepared for each experiment and kept on ice.

Acknowledgments

This work was supported by grants from the DOE, NIH, and ONR. G.M. holds an M.D.-Ph.D. fellowship in the Medical Scientist Training Program at The Texas A&M University System Health Science Center and was the recipient of an ASSERT (ARO) award. The authors thank Stephen Cheley, Orit Braha, and Li-Qun Gu for discussions, Brian Lauman for technical assistance, and Sean Conlan and Gay Pridgeon for graphics.

The publication costs of this article were defrayed in part by payment of page charges. This article must therefore be hereby marked "advertisement" in accordance with 18 USC section 1734 solely to indicate this fact.

References

Abrahams, J.P., Leslie, A.G.W., Lutter, R., and Walker, J.E. 1994. Structure at 2.8Å resolution of F_1-ATPase from bovine heart mitochondria. *Nature* **370:** 621–628.

Alouf, J.E. and J.H. Freer. 1999. *The comprehensive sourcebook of bacterial protein toxins*, 2nd ed. Academic Press, San Diego, CA, p. 718.

Archibald, J.M., Logsdon, J.M., and Doolittle, W.F. 2000. Origin and evolution of eukaryotic chaperonins: Phylogenetic evidence for ancient duplications in CCT genes. *Mol. Biol. Evol.* **17:** 1456–1466.

Baida, G., Budarina, Z.I., Kuzmin, N.P., and Solonin, A.S. 1999. Complete nucleotide sequence and molecular characterization of hemolysin II gene from *Bacillus cereus*. *FEMS Microbiol. Lett.* **180:** 7–14.

Bayley, H. 1997. Toxin structure: Part of a hole? *Current Biol.* **7:** R763-R767.

———. 1999. Designed membrane channels and pores. *Curr. Opin. Biotechnol.* **10:** 94–103.

Bayley, H. and Cremer, P.S. 2001. Stochastic sensors inspired by biology. *Nature* **413:** 226–230.

Bhakdi, S., Walev, I., Palmer, M., and Valeva, A. 2000. Staphylococcal α toxin. In *Bacterial protein toxins* (eds. K. Aktories and I. Just), pp. 509–527. Springer, Berlin.

Braha, O., Walker, B., Cheley, S., Kasianowicz, J.J., Song, L., Gouaux, J.E., and Bayley, H. 1997. Designed protein pores as components for biosensors. *Chem. Biol.* **4:** 497–505.

Bronner, S., Stoessel, P., Gravet, A., Monteil, H., and Prévost, G. 2000. Variable expressions of *Staphylococcus sureus* bicomponent leucotoxins semiquantified by competitive reverse transcription PCR. *Appl. Env. Microbiol.* **66:** 3931–3938.

Cheley, S., Malghani, M.S., Song, L., Hobaugh, M., Gouaux, J.E., Yang, J., and Bayley, H. 1997. Spontaneous oligomerization of a staphylococcal α-hemolysin conformationally constrained by removal of residues that form the transmembrane β barrel. *Protein Eng.* **10:** 1433–1443.

Cheley, S., Braha, O., Lu, X., Conlan, S., and Bayley, H. 1999. A functional protein pore with a 'retro' transmembrane domain. *Protein Sci.* **8:** 1257–1267.

Christopher, J.A. 1998. *SPOCK: The structural properties observation and calculation kit (program manual)*. Center for Macromolecular Design, Texas A&M University, College Station, TX.

Cooney, J., Mulvey, M., Arbuthnott, J., and Foster, T. 1988. Molecular cloning and genetic analysis of the determinant for γ-lysin, a two component toxin of *Staphylococcal aureus*. *J. Gen. Microbiol.* **134:** 2179–2188.

Cooney, J., Kienle, Z., Foster, T.J., and O'Toole, P.W. 1993. The γ-hemolysin locus of *Staphylococcus aureus* comprises three linked genes, two of which are identical to the genes for the F and S components of leukocidin. *Infect. Immun.* **61:** 768–771.

Czajkowsky, D.M., Sheng, S., and Shao, Z. 1998. Staphylococcal α-hemolysin can form hexamers in phospholipid bilayers. *J. Mol. Biol.* **276:** 325–330.

Eroglu, A., Russo, M.J., Bieganski, R., Fowler, A., Cheley, S., Bayley, H., and Toner, M. 2000. Intracellular trehalose improves the survival of cryopreserved mammalian cells. *Nature Biotechnol.* **18:** 163–167.

Fang, Y., Cheley, S., Bayley, H., and Yang, J. 1997. The heptameric prepore of a staphylococcal α-hemolysin mutant in lipid bilayers imaged by atomic force microscopy. *Biochemistry* **36:** 9518–9522.

Ferreras, M., Höper, F., Dalla Serra, M., Colin, D.A., Prévost, G., and Menestrina, G. 1998. The interaction of *Staphylococcus aureus* bi-component γ-hemolysins and leucocidins with cells and lipid membranes. *Biochim. Biophys. Acta* **1414:** 108–126.

Gouaux, E. 1998. α-Hemolysin from *Staphylococcus aureus*: An archetype of β-barrel, channel-forming toxins. *J. Struct. Biol.* **121:** 110–122.

Gouaux, J.E., Braha, O., Hobaugh, M.R., Song, L., Cheley, S., Shustak, C., and Bayley, H. 1994. Subunit stoichiometry of staphylococcal α-hemolysin in crystals and on membranes: A heptameric transmembrane pore. *Proc. Natl. Acad. Sci.* **91:** 12828–12831.

Gouaux, E., Hobaugh, M., and Song, L. 1997. α -Hemolysin, γ-hemolysin and leukocidin from *Staphylococcus aureus*: Distant in sequence but similar in structure. *Protein Sci.* **6:** 2631–2635.

Gravet, A., Colin, C.A., Keller, D., Giradot, R., Monteil, H., and Prévost, G. 1998. Characterization of a novel structural member,LukE-LukD, of the bi-component staphylococcal leucotoxins family. *FEBS Lett.* **436:** 202–208.

Harrison, S.C. 2001. The familiar and the unexpected in structures of icosahedral viruses. *Curr. Opin. Struct. Biol.* **11:** 195–199.

Heginbotham, L., Odessey, E., and Miller, C. 1997. Tetrameric structure of a prokaryotic K^+ channel. *Biochemistry* **36:** 10335–10342.

Heuck, A.P., Tweten, R.K., and Johnson, A.E. 2001. β-Barrel pore-forming toxins: Intriguing dimorphic proteins. *Biochemistry* **40:** 9065–9073.

Howorka, S. and Bayley, H. 1998. Improved protocol for high-throughput cysteine scanning mutagenesis. *Biotechniques* **25:** 766–772.

Howorka, S., Cheley, S., and Bayley, H. 2001. Sequence-specific detection of individual DNA strands using engineered nanopores. *Nature Biotechnol.* **19:** 636–639.

Jiang, W., Hermolin, J., and Fillingame, F.H. 2001. The preferred stoichiometry of c subunits in the rotary motor section of *Escherichia coli* ATP synthase is 10. *Proc. Natl. Acad. Sci.* **98:** 4966–4971.

Jones, D.H. 1995. PCR mutagenesis and recombination in vivo. In *PCR primer: A laboratory manual* (eds. C.W. Dieffenbach and G.S. Dveksler). Cold Spring Harbor Laboratory Press, Cold Spring Harbor, NY.

Kaneko, J., Ozawa, T., Tomita, T., and Kamio, Y. 1997. Sequential binding of staphylococcal γ-hemolysin to human erythrocytes and complex formation of hemolysin on the cell surface. *Biosci. Biotech. Biochem.* **61:** 846–851.

Karlin, A. 1993. Structure of nicotinic acetylcholine receptors. *Curr. Opin. Neurobiol.* **3:** 299–309.

König, B., Prévost, G., and König, W. 1997. Composition of staphylococcal

bi-component toxins determines pathophysiological reactions. *J. Med. Microbiol.* **46:** 479–485.

Krasilnikov, O.V., Merzlyak, P.G., Yuldasheva, L.N., Rodrigues, C.G., Bhakdi, S., and Valeva, A. 2000. Electrophysiological evidence for heptameric stoichiometry of ion channels formed by *Staphylococcus aureus* α-toxin in planar lipid bilayers. *Mol. Microbiol.* **37:** 1372–1378.

Laemmli, U.K. 1970. Cleavage of structural proteins during the assembly of the head of bacteriophage T4. *Nature* **227:** 680–685.

Menestrina, G., Dalla Serra, M., and Prévost, G. 2001. Mode of action of β barrel pore-forming toxins of the staphylococcal α-hemolysin family. *Toxicon* **39:** 1661–1672.

Merritt, E.A. and Murphy, M.E.P. 1994. Raster3D version 2.0—A program for photorealistic molecular graphics. *Acta Crystallogr.* **D50:** 869–873.

Miles, G., Cheley, S., Braha, O., and Bayley, H. 2001. The staphylococcal leukocidin bicomponent toxin forms large ionic channels. *Biochemistry* **40:** 8514–8522.

Miyata, S., Matsushita, O., Minami, J., Katayama, S., Shimamoto, S., and Okabe, A. 2001. Cleavage of a C-terminal peptide is essential for heptamerization of *Clostridium perfringens* ε-toxin in the synaptosomal membrane. *J. Biol. Chem.* **276:** 13778–13783.

Montal, M. and Mueller, P. 1972. Formation of bimolecular membranes from lipid monolayers and study of their electrical properties. *Proc. Natl. Acad. Sci.* **69:** 3561–3566.

Movileanu, L., Howorka, S., Braha, O., and Bayley, H. 2000. Detecting protein analytes that modulate transmembrane movement of a polymer chain within a single protein pore. *Nature Biotechnol.* **18:** 1091–1095.

Movileanu, L., Cheley, S., Howorka, S., Braha, O., and Bayley, H. 2001. Location of a constriction in the lumen of a transmembrane pore by targeted covalent attachment of polymer molecules. *J. Gen. Physiol.* **117:** 239–251.

Murzin, A.G., Lesk, A.M., and Chothia, C. 1994a. Principles determining the structure of β-sheet barrels in proteins I. A theoretical analysis. *J. Mol. Biol.* **236:** 1369–1381.

———. 1994b. Principles determining the structure of β-sheet barrels in proteins II. The observed structures. *J. Mol. Biol.* **236:** 1382–1400.

Olson, R., Nariya, H., Yokota, K., Kamio, Y., and Gouaux, E. 1999. Crystal structure of staphylococcal LukF delineates conformational changes accompanying formation of a transmembrane channel. *Nature Struct. Biol.* **6:** 134–140.

Ozawa, T., Kaneko, J., and Kamio, Y. 1995. Essential binding of LukF of staphylococcal γ-hemolysin followed by the binding of HγII for the hemolysis of human erythrocytes. *Biosci. Biotech. Biochem.* **59:** 1181–1183.

Pédelacq, J.-D., Maveyraud, L., Prévost, G., Baba-Moussa, L., González, A., Courcelle, E., Shepard, W., Monteil, H., Samama, J.-P., and Mourey, L. 1999. The structure of *Staphylococcus aureus* leukocidin component (LukF-PV) reveals the fold of the water-soluble species of a family of transmembrane pore-forming toxins. *Structure* **7:** 277–288.

Prévost, G., Cribier, B., Couppié, P., Petiau, P., Supersac, G., Finck-Barbançon, V., Monteil, H., and Piémont, Y. 1995. Panton-Valentine leucocidin and γ-hemolysin from *Staphylococcus aureus* ATCC 49775 are encoded by distinct genetic loci and have different biological activities. *Infect. Immun.* **63:** 4121–4129.

Rohrwild, M., Pfeifer, G., Santarius, U., Muller, S.A., Huang, H.C., Engel, A., Baumeister, W., and Goldberg, A.L. 1997. The ATP-dependent Hs1VU protease from *Escherichia coli* is a four-ring structure resembling the proteasome. *Nat. Struct. Biol.* **4:** 133–139.

Seelert, H., Poetsch, A., Dencher, N.A., Engel, A., Stahlberg, H., and Müller, D.J. 2000. Proton-powered turbine of a plant motor. *Nature* **405:** 418–419.

Song, L., Hobaugh, M.R., Shustak, C., Cheley, S., Bayley, H., and Gouaux, J.E. 1996. Structure of staphylococcal α-hemolysin, a heptameric transmembrane pore. *Science* **274:** 1859–1865.

Stahlberg, H., Muller, D.J., Suda, K., Fotiadis, D., Engel, A., Meier, T., Matthey, U., and Dimroth, P. 2001. Bacterial Na^+-ATP synthase has an undecameric rotor. *EMBO Rep.* **2:** 229–233.

Stock, D., Leslie, A.G.W., and Walker, J.E. 1999. Molecular architecture of the rotary motor in ATP synthase. *Science* **286:** 1700–1705.

Sugawara, N., Tomita, T., and Kamio, Y. 1997. Assembly of *Staphylococcus aureus* γ-hemolysin into a pore-forming ring-shaped complex on the surface of human erythrocytes. *FEBS Lett.* **410:** 333–337.

Sugawara, N., Tomita, T., Sato, T., and Kamio, Y. 1999. Assembly of *Staphylococcus aureus* leukocidin into a pore-forming ring-shaped oligomer on human polymorphonuclear leukocytes and rabbit erythrocytes. *Biosci. Biotech. Biochem.* **63:** 884–891.

Thompson, J.D., Higgins, D.G., and Gibson, T.J. 1994. CLUSTAL W: Improving the sensitivity of progressive multiple sequence alignment through sequence weighting, positions-specific gap penalties and weight matrix choice. *Nucleic Acids Res.* **22:** 4673–4680.

Walker, B.J., Krishnasastry, M., Zorn, L., and Bayley, H. 1992. Assembly of the oligomeric membrane pore formed by staphylococcal α-hemolysin examined by truncation mutagenesis. *J. Biol. Chem.* **267:** 21782–21786.

Walker, B., Braha, O., Cheley, S., and Bayley, H. 1995. An intermediate in the assembly of a pore-forming protein trapped with a genetically-engineered switch. *Chem. Biol.* **2:** 99–105.

Zitzer, A., Zitzer, O., Bhakdi, S., and Palmer, M. 1999. Oligomerization of Vibrio cholera cytolysin yields a pentameric pore and has a dual specificity for cholesterol and sphingolipids in the target membrane. *J. Biol. Chem.* **274:** 1375–1380.